

An Exposition of Pathfinding Strategies Within Lightning Network Clients

Sindura Saraswathi

Department of Computer Science
University of North Carolina at Charlotte
Charlotte, NC, USA
ssarasw2@charlotte.edu

Christian Kümmerle

Department of Computer Science
University of North Carolina at Charlotte
Charlotte, NC, USA
kummerle@charlotte.edu

Abstract—The Lightning Network is a peer-to-peer network designed to address Bitcoin’s scalability challenges, facilitating rapid, cost-effective, and instantaneous transactions through bidirectional, blockchain-backed payment channels among network peers. Due to a source-based routing of payments, different pathfinding strategies are used in practice, trading off different objectives for each other such as payment reliability and routing fees. This paper explores differences within pathfinding strategies used by prominent Lightning Network node implementations, which include different underlying cost functions and different constraints, as well as different greedy algorithms of shortest path-type. Surprisingly, we observe that the pathfinding problems that most LN node implementations attempt to solve are NP-complete, and cannot be guaranteed to be optimally solved by the variants of Dijkstra’s algorithm currently deployed in production. Through comparative analysis and simulations, we evaluate efficacy of different pathfinding strategies across metrics such as success rate, fees, path length, and timelock. Our experiments indicate that the strategies used by LND tend to be advantageous in terms of payment reliability, Eclair tends to result in paths with low fees, and that LDK exhibits average reliability with larger fee levels for smaller payment amounts; furthermore, CLN stands out for its minimal timelock paths. Additionally, we investigate the impact of Lightning node connectivity levels on routing efficiency. The findings of our analysis provide insights towards future improvements of pathfinding strategies and algorithms used within the Lightning Network.

I. INTRODUCTION AND BACKGROUND

Bitcoin [1], the world’s first and arguably dominant decentralized digital currency, operates on a peer-to-peer network which allows transactions to be recorded securely on a distributed public ledger, also known as the blockchain, and to be verified individually, without the need for trusted third parties. However, Bitcoin encounters scalability challenges attributable to its existing block size limitations, which are challenging to overcome without compromising the decentralization or the security [2], [3] of the network. To address the scalability challenges inherent in Bitcoin, the Lightning Network (LN) [4], an off-chain payment channel network, was proposed in 2016.

By leveraging the trust and security of the Bitcoin blockchain in its payment channels, the Lightning Network offers bitcoin-denominated fast, cost-effective, and scalable transactions. Within the LN, users establish bidirectional payment channels, which collectively form a peer-to-peer network.

These channels operate as 2-of-2 multisignature contracts between two parties (nodes) that hold bitcoin. Through these channels, users, which serve as nodes within the LN, can conduct off-chain transactions. Settlement of these off-chain transactions on the Bitcoin blockchain occurs only when necessary, such as when a user opts to close a channel. This architecture renders the Lightning Network scalable and enables instant payments [5].

Two channel peers lock a certain amount of bitcoins into a 2-of-2 multisignature address, constituting the total capacity of the channel. Each peer possesses a portion of this total capacity, which they can spend. This spendable portion held by each channel peer is referred to as their channel balance or channel liquidity. As transactions occur within the channel, these balances may fluctuate. Depending on the direction of payments, one peer’s balance will decrease while the other peer’s balance increases [6].

The payment channel enables two nodes to conduct numerous transactions within the channel in both directions by generating revocable commitment transactions, thus eliminating the need for them to be broadcast on the blockchain [7]. However, to securely route payments across multiple hops from the source to the destination, Hashed Timelock Contracts (HTLCs) are used [4].

Multi-hop payments are facilitated through source routing, wherein the source locates a path to the receiver for payment routing. Initially, the sender receives a cryptographic hash from the recipient. For the sender’s payment to succeed, the recipient, upon receiving the HTLC, must return the pre-image along the HTLC-routed path within a specified timelock. Consequently, upon payment initiation, a series of HTLCs are established along the intended path. Each HTLC represents a commitment of funds from the preceding node to the next node, contingent upon the fulfillment of cryptographic proof. Once all contracts are established, the receiver shares the pre-image of the hash with its predecessor hop, which forwards it along the path until it reaches the sender, thereby resolving HTLCs along the path [8]. LN nodes can route payments only if they have sufficient balance on their side of the channel. A key practical challenge for successful payments within the LN is that the sender node selecting a payment path only possesses information about the capacity of channels, but not about the

balance distribution within them [9], which might lead to the selection of payment path that cannot successfully route the payment amount.

In order to discover paths for routing payments, the sender node utilizes a pathfinding algorithm. Popular and widely used pathfinding algorithms have been developed by various LN implementations, including Lightning Network Daemon (LND) [10], Core Lightning (CLN) [11], Lightning Development Kit (LDK) [12], and Eclair [13]. While mostly using a variant of a shortest-path algorithm, each of these node implementations differs in its pathfinding strategy in substantial details such as in the weight function that establishes underlying path costs. With their different choices, these LN client implementations adopt diverse approaches to the pathfinding process with different trade-offs regarding the fees incurred by payments, the typical length of payment paths, incurred delays and payment reliability. Only little research has been dedicated to selecting the appropriate client (or pathfinding strategy) based on different need profiles regarding these trade-offs inherent to payment delivery within LN.

In this paper, we present a comprehensive analysis of the single-path pathfinding algorithms deployed by LND, CLN, LDK, and Eclair. Our objective is to compare the underlying channel weight functions, constraints, properties of deployed algorithms, and evaluate the performance and reveal the strengths and weaknesses of each client variant, providing insights for LN developers and researchers to guide future research and development efforts.

We discuss related works in Section II, followed by an explanation of the pathfinding process within LN in Section III. In Section IV, we examine design elements of weight functions used in shortest path algorithms. We then present details on the pathfinding algorithms used by LN clients in Section V, discussing also additionally imposed constraints, and provide a counterexample for the optimality of the modified Dijkstra variant used in LND for their imposed cost function. Section VI delves into the discussion of implementation of pathfinding and weight functions used by different LN clients. We present our simulation model, experimental setup, results, and analysis in Section VII. Section VIII discusses the limitations of our study. Finally, we conclude this paper in Section IX.

II. RELATED WORK

Numerous studies have examined off-chain payment channel networks like the Lightning Network, encompassing evaluations of network topology, enhancements to routing schemes, and considerations of security and reliability.

The study by [14] concentrates on the reliability and privacy of LN payments by introducing a mathematical framework to model uncertainty in channel balances using probability theory. Furthermore, [15] explores the privacy properties of the Lightning Network through simulations. [16] investigates the structure of the Lightning Network and the routing algorithms used by LND, CLN and Eclair. It then explores the effects

of routing choices by analyzing the feasibility of Denial-of-Service attacks and route hijacking across these three implementations. In our work, we specifically analyze the effects of design elements in the pathfinding algorithm and evaluate their empirical performance from an operational perspective.

[17] examines the potential presence of the Braess paradox in off-chain networks and proposes solutions to mitigate its impact through analysis employing three routing algorithms, including LND and CLN. [18] analyzes the Lightning Network's topology and introduces a strategy called ProfitPilot for connecting new nodes in payments by encouraging cycle creation in payment channel networks. Studies such as [19], [15], and [20] present topological analyses of the Lightning Network. In our study, we utilize insights into the Lightning Network topology, including the node connectivity levels, to analyze the performance of pathfinding strategies for different network participants.

While our research focuses on existing implementations of single-path pathfinding strategies within the current LN protocol, several studies have proposed modifications to the routing protocol that go beyond the current capabilities of LN. Flare [21] proposes a routing methodology in the Lightning Network that relies on routing tables and beacon nodes to determine paths. Spider [22] presents a routing solution that segments transactions into packets and utilizes a multi-path transport protocol to ensure balanced channel usage. Boomerang [23] introduces redundant payments on existing multi-path routing schemes to reduce latency.

Beyond the scope of our exposition are payment delivery strategies based on (atomic) multi-part payments [6, Chapter 12], which have been introduced as an extension to the original LN protocol [24]. [25] argues that multipart payment delivery benefits from integrating payment probability and the formulation via minimum cost flows instead of following a shortest-path framework. [26] proposes a variation of Boomerang which requires less computing power and latency for faster multi-path payments. While multi-part payments are very promising, they do currently not (yet) represent the mainstream practice in LN, where single-path payments still dominate. Thus, our study focuses on single-path payments, but the conducted analysis could be extended to multi-part payments in future work.

A paper with a similar scope as our exposition is [8], which undertakes a comparative examination of routing clients, analyzing weight functions of LND, CLN, and Eclair. However, significant developments and enhancements have occurred in these routing clients since that study, and [8] does not consider constraints or modification of Dijkstra's algorithm which are necessary to account for certain choices of cost functions, e.g., the ones used by LND. As an additional routing client, our research also includes LDK alongside these clients. The distinct experimental methodology to evaluate the performance of different pathfinding strategies is further different than that of [8], as we also consider different connectivity levels of nodes. Finally, the systematic analysis of weight function design elements as presented in Section IV is novel to the

best of our knowledge.

III. PATHFINDING AND ROUTE SELECTION

For the purpose of pathfinding, the Lightning Network can be modelled as a directed graph $G = (V, E)$, in which each network participant is represented as a node or vertex $v \in V$, and a payment channel between two nodes $u, v \in V$ is represented as the pair of edges $e = (u, v) \in E$ and $e = (v, u) \in E$. Each edge in the graph is associated with specific channel attributes such as fees, capacity, timelock delta, age, and information amount the maximal and minimal amount of currency units that can be settled in an HTLC. These channel attributes are also utilized as design elements for pathfinding purposes. It is important to note that the LN graph evolves dynamically over time—the number of nodes and channels changes through channel opening and closing transactions, and beyond that, node operators adapt channel parameters such as fee parameters and communicate those changes via a gossip protocol to other network participants.

In LN transactions, the node that initiates the payment is often referred to as the source node, while the node that receives the payment is called the destination or receiver node. There are several intermediary nodes that facilitate the forwarding of payments between the source and receiver nodes. These intermediary nodes are commonly referred to as routing nodes, and the channels included in this payment forwarding are referred to as hops.

When the payment is initiated, the source node needs to find a path to the receiver node using pathfinding strategies on the LN graph. Existing LN clients employ instantiations of shortest path algorithms, such as Dijkstra’s algorithm, modified Dijkstra-style algorithms or Yen’s K -shortest path algorithm, to find the path between specified source and receiver nodes [27], [28], [29] and [30]. We refer to Section V for a discussion of these variants in the context of their use in LN implementations.

IV. WEIGHT FUNCTION DESIGN ELEMENTS

Given the a sender node $s \in V$ and a recipient node $r \in V$, shortest path algorithms aim to find a path $p = (e_1, \dots, e_{\text{length}(p)})$ of edges $e_i \in E$, where s is the initial node of e_1 and r is the terminal node of $e_{\text{length}(p)}$, which minimizes a total path cost $c(p)$ given as the sum of *edge weights* given by a function $\text{weight} : E \rightarrow \mathbb{R}_{\geq 0}$ that maps to non-negative real numbers $\mathbb{R}_{\geq 0}$, such that

$$c(p) := \sum_{i=1}^{\text{length}(p)} \text{weight}(e_i) = \sum_{e \in p} \text{weight}(e), \quad (1)$$

cf. [31, Chapter 22]. Recalling that an edge in the LN graph corresponds to a payment channel, this means that current LN client implementations, which use the shortest path algorithms to find their payment paths (see Section V), implicitly assume additive path costs in the sense of (1).

Depending on different design choices that are made, the edge weight function $\text{weight}(\cdot)$ is composed of different

terms, which try to capture different desired properties of the resulting payment path returned by the pathfinding algorithm. Specifically, in the following, we model the edge weight function to have the form

$$\text{weight}(e) = \sum_{i=1}^k c^i a_e^i, \quad (2)$$

where k is a number of distinct elementary weight terms, $a_e^i \geq 0$ is an edge-specific factor associated to the i -th weight term, and $c^i \geq 0$ is an associated factor or constant that does not depend on the edge e in consideration.

However, the choice of these factors c^i and a_e^i varies across the clients. In this section, we examine various design components and concepts contributing to weight functions of LN clients, with a specific focus on discussing the principles and model assumptions underlying these components. The usage of each of these elements can lead to payment paths exhibiting a variety of different properties.

A. Fees

When routing payments from a source s to a recipient node r , the payment path p typically involves intermediary nodes and multiple hops. These intermediary nodes charge fees for each successfully settled transaction they participate in. These fees can be subdivided into two distinct parts: the base fee (b_e), which remains constant regardless of the transaction size, and the proportional fee or fee rate (f_e), which varies based on the amount being forwarded through the node. Consequently, the total fee charged by an intermediary node for forwarding a specific payment amount (amt_e) is determined by the combination of these two components, such that

$$\text{fee}_e = b_e + \text{amt}_e \cdot f_e. \quad (3)$$

Since it is reasonable for the source node to try to find a path with fees as low as possible, one of the weight terms a_e^i in (2) can be chosen as $a_e^i = \text{fee}_e$ defined above. This choice is a primary design consideration in all LN implementations when formulating their weight functions. Since fees are directional, i.e., they can vary depending on the direction of payment flow between the same two nodes $u, v \in V$, a modeling of the LN as a directed graph instead of an undirected one is more appropriate.

B. Timelock

Once a specific number of blocks is reached — referred to as a timelock — each incoming HTLC in a channel expires. This timelock serves as a time buffer within which the node aims to complete all the HTLC exchanges for a given transaction. For the length of the timelock, funds are locked in the payment channels.

The total timelock of an HTLC, in direction from sender to recipient, depends on the timelock of the subsequent HTLC along a payment path plus the timelock difference value Δ_e^{CLTV} , called *timelock delta* or *CLTV expiry delta*¹ that is set

¹CLTV is an acronym of the Bitcoin script operator OP_CHECKLOCKTIMEVERIFY [6, Glossary].

by the node v at the outgoing side of the channel $e = (u, v)$ [6, Chapter 8]. In order to ensure that funds are locked for a shorter duration, it is reasonable for routing clients to prioritize the inclusion of channels with lower timelock deltas into the payment path compared to channels with higher timelock deltas.

For this reason, to penalize channel with large timelock deltas, a weight term a_e^i in (2) can be chosen to be proportional to the timelock delta Δ_e^{CLTV} . In LND, CLN, and Eclair, an edge-dependent proportionality factor is chosen such that $a_e^i = \text{amt}_e \cdot \Delta_e^{\text{CLTV}}$. The corresponding constant, potentially tunable factor c_i is called riskfactor in LND and CLN and lockedFundsRisk in Eclair. In LDK, an upper bound on the timelock delta is used as a constraint for a channel to be considered during pathfinding, but it does not appear as part of a weight term.

C. Success Probability

Due to the fact that payment paths in which the desired payment amount can be settled reliably are preferred, it is common to take an estimate of a success probability, which estimates the likelihood of a successful payment through a payment path, into account when searching for suitable payment paths p . In this subsection, we first discuss two different approaches for incorporating payment path success probabilities into a model for a total path cost, and then shed light on different approaches for modelling individual channel success probabilities.

1) *Path Success Probability*: Given a path p between sender node $s \in V$ and recipient node $r \in V$, assume that we have access to an estimate $P_p \in [0, 1]$ for its success probability.

In existing literature on LN pathfinding, there are two different approaches for incorporating a path success probability estimate P_p into a total path cost $c(p)$ of a payment path p .

The first, which is used in LND [32], [33] implies a success probability penalization that is proportional to the inverse P_p^{-1} of the path success probability P_p . It is based on the following derivation.

Lemma IV.1. *Assume that we compare two paths a and b between sender $s \in V$ and recipient $r \in V$ which incur a fee cost (e.g., incurred routing fee) of F_a and F_b , respectively, if successfully used to route the payment. Assume that an additional fixed virtual cost c_{attempt} is incurred for a payment attempt along any path p .² Then, the expected total cost after two payment attempts is minimized by trying first the path p which is a minimizer of the objective*

$$c(p) = F_p + \frac{c_{\text{attempt}}}{P_p} + c_0, \quad (4)$$

where $c_0 \in \mathbb{R}$ is an arbitrary, path-independent constant.

Proof. If path a is tried and succeeds, a cost of $F_a + c_{\text{attempt}}$ is incurred. On the other hand, if path a is tried and does not succeed, there are two possible outcomes: Either the subsequently path b succeeds, in which case a total cost of

$F_b + 2c_{\text{attempt}}$ is incurred, or subsequent path b fails, in which a total cost of $2c_{\text{attempt}}$ is incurred.

The cost c_{ab} of attempting to use first path a and then b is thus in expectation

$$\begin{aligned} \mathbb{E}[c_{ab}] &= P_a(F_a + c_{\text{attempt}}) + (1 - P_a)P_b(F_b + 2c_{\text{attempt}}) \\ &\quad + (1 - P_a)(1 - P_b)2c_{\text{attempt}}, \end{aligned}$$

whereas the cost c_{ba} of attempting to use first path b and then a is in expectation

$$\begin{aligned} \mathbb{E}[c_{ba}] &= P_b(F_b + c_{\text{attempt}}) + (1 - P_b)P_a(F_a + 2c_{\text{attempt}}) \\ &\quad + (1 - P_b)(1 - P_a)2c_{\text{attempt}}. \end{aligned}$$

In both cases, the outcome regarding payment success is the same—if any of the two paths a and b is able to route the payment successfully, the payment will be successful, otherwise, the payment has failed. Thus, it is sufficient to compare $\mathbb{E}[c_{ab}]$ with $\mathbb{E}[c_{ba}]$ to obtain a preference for a over b or vice versa. In particular, we see that $\mathbb{E}[c_{ab}] < \mathbb{E}[c_{ba}]$ is equivalent to

$$\begin{aligned} P_a c_{\text{attempt}} - 2P_a P_b c_{\text{attempt}} - P_a P_b F_b + 2P_b c_{\text{attempt}} \\ < P_b c_{\text{attempt}} - 2P_a P_b c_{\text{attempt}} - P_a P_b F_a + 2P_a c_{\text{attempt}}, \end{aligned}$$

which holds if and only if

$$\begin{aligned} P_a P_b F_a + P_b c_{\text{attempt}} \\ < P_a P_b F_b + P_a c_{\text{attempt}}. \end{aligned}$$

If neither success probability P_a nor P_b is 0, via multiplication by $\frac{1}{P_a P_b}$, this is equivalent to

$$F_a + \frac{c_{\text{attempt}}}{P_a} + c_0 < F_b + \frac{c_{\text{attempt}}}{P_b} + c_0,$$

for any $c_0 \in \mathbb{R}$, which shows that choosing $p \in \{a, b\}$ minimizing (4) leads to the desired outcome. If either $P_a = 0$ or $P_b = 0$, minimizing (4) also leads to the desired outcome as (4) corresponds to an infinite expected total cost for $P_p = 0$, but a finite expected total cost for any path with non-zero P_p . \square

We note that in [32], [33], the derivation above is conducted assuming the existence of a virtual cost c_{attempt} only in case of a payment failure, but both assumptions lead to the same objective (4). In (4), the fee cost term F_p fits well into the additive framework of (1) due the fact that routing fees accumulate additively along the path such that $F_p = \sum_{e \in p} \text{weight}_a(e)$, where $\text{weight}_a : E \rightarrow \mathbb{R}_{\geq 0}$ is a non-negative, additive weight function.

However, for second summand of (4), the situation is different as an additive decomposition of $\frac{c_{\text{attempt}}}{P_p}$ across edges can be mathematically not justified. On the other hand, a reasonable assumption is that a payment across a path p is successful if and only if the routing across *all* channels $e \in p$ is successful, who themselves are assigned channel success probabilities P_e . If we assume that the routing success across

²See also Section IV-D.

one channel $e \in p$ is independent from the routing success across any other channels along each path, we have that

$$\begin{aligned} P_p &= P(\{\text{payment across path } p \text{ is successful}\}) \\ &= P(\cap_{e \in p} \{\text{payment across channel } e \text{ is successful}\}) \\ &= \prod_{e \in p} P_e, \end{aligned}$$

using the independence assumption in the last equality. In view of this equality, it is possible to decompose the cost of (4) across edges if we introduce the multiplicative weight $\text{weight}_m : E \rightarrow \mathbb{R}_{\geq 1}, e \mapsto 1/P_e$ such that, in the case of $c_0 = 0$,

$$c(p) = F_p + \frac{c_{\text{attempt}}}{P_p} = \underbrace{\sum_{e \in p} \text{weight}_a(e)}_{=:c_a(p)} + \underbrace{c_{\text{attempt}} \prod_{e \in p} \text{weight}_m(e)}_{=:c_m(p)}. \quad (5)$$

Unfortunately, it is not possible to use a standard shortest path algorithm such as Dijkstra's algorithm to find the path with the lowest additive-plus-multiplicative cost (5) as these algorithms all assume additive cost as in (1) [31, Chapter 22].

The LND LN node implementation mitigates this issue by modifying the priority queue used in Dijkstra's algorithm to be adapted to (5). However, as we discuss in Section V, it can be shown that such a modified Dijkstra is not guaranteed to find the optimal path with respect to (5).

A second approach to incorporate the path success probability P_p into a path cost function is to add a factor proportional to $\log\left(\frac{1}{P_p}\right)$ instead of $\frac{1}{P_p}$. Under the independence assumption of the payment across path edges e mentioned above, we see that

$$\log\left(\frac{1}{P_p}\right) = -\log\left(\prod_{e \in p} P_e\right) = -\sum_{e \in p} \log(P_e), \quad (6)$$

which leads to a fully additive cost of the type (1) motivates the choice of a weight term $a_e^i = -\log(P_e)$ in (2). Since the edge success probabilities P_e are between 0 and 1, these weight terms are always non-negative. If used without any other weight terms (e.g., fee-related ones), the resulting problem type corresponds to finding a *maximally reliable path* and is known to be equivalent to a shortest path problem [34, Exercise 4.39]. CLN, LDK and Eclair use this logarithmic success probability term in their weight function to prioritize paths with higher success probability within their pathfinding algorithms.

Comparing the two approaches, we note that while an inverse penalization P_p leads to difficulties in the pathfinding algorithms as mentioned above, an argument can be made that this modeling is more suitable to avoid unreliable paths as $1/P_p$ grows faster for $P_p \rightarrow 0$ than $-\log(P_p)$, i.e., the penalization of unreliable vs. reliable paths is stronger in the modeling used by LND.

2) *Channel-Wise Success Probability*: We discussed in the last subsection how, through considering path success probabilities and a suitable independence assumption, weight terms

based on P_e , the probability that the channel e is able to successfully route a payment, are suitable design elements within total path costs (1). There are different approaches to estimate this channel-wise success probability P_e , underlying different assumptions.

As a simple, first approach, every untried channel can be assumed to have a constant default success probability [33]. For channels used in routing payments historically, the success probability estimation can be based on the outcomes of historical payment attempts [10]. If historical payment data is collected across many payment attempts, in the event of a failed payment attempt, the channel success probability estimate P_e can be decreased to 0. The channel success probability estimate P_e gradually returns to its default value over time.

In LND, there are two ways to calculate the channel's success probability: *Apriori* and *Bimodal*. This approach is followed in LND's *Apriori* mode.

Another popular model to estimate P_e is based on modeling the relationship between the intended payment amount and the channel capacity [13]. Capacity is the sum of balances across the nodes in the channel. While channel's capacity is publicly known, the individual balances remain private. A large channel capacity relative to the payment amount intuitively leads to greater probability of success, which is why it can be used within a success probability estimate. Specifically, assuming a uniform distribution for channel liquidity, the failure probability can be expressed as the ratio of payment amount amt_e to the channel capacity cap_e , such that the success probability P_e can be written as

$$P_e = 1 - \frac{\text{amt}_e}{\text{cap}_e} = \frac{\text{cap}_e - \text{amt}_e}{\text{cap}_e}.$$

In this modeling, the success probability P_e decreases as the payment amount approaches the channel's capacity. This model is used in Eclair.

Based on the same assumption, a finer model for P_e can be obtained if upper and lower bounds UB_e and LB_e for the available balance (or liquidity) in a channel e are available, as mentioned in [12]. This approach to model the channel success probability is inspired by [14]. If it is known that the (unknown) liquidity balance x satisfies $\text{LB}_e \leq x < \text{UB}_e$, under a uniform probability assumption, it holds that $P(x = b) = \frac{1}{\text{UB}_e - \text{LB}_e}$ for any b with $\text{LB}_e \leq b < \text{UB}_e$, which implies that we can model the probability that a payment of size amt_e through channel e fails as $P(x < \text{amt}_e) = \sum_{b=\text{LB}_e}^{\text{amt}_e-1} P(x = b) = \frac{\text{amt}_e - \text{LB}_e}{\text{UB}_e - \text{LB}_e}$. Therefore, the success probability can be expressed as

$$P_e = P(x \geq \text{amt}_e) = 1 - P(x < \text{amt}_e) = \frac{\text{UB}_e - \text{amt}_e}{\text{UB}_e - \text{LB}_e}.$$

CLN and LDK use this approach by assigning default values to the upper and lower bounds of liquidity in a channel based on its capacity. Additionally, in LDK, these bounds are adjusted based on the outcomes of many payment attempts. However, the adjusted bounds gradually revert to their default values over time.

While the previous approaches are based on the assumption of uniform liquidity distribution, assuming a bimodal liquidity distribution is more practical, as the channel liquidity is often unbalanced due to unidirectional flows from the strong sources to strong recipients. This results in liquidity being concentrated either on the local or the remote side [35]. Therefore, the success probability estimation can be based on the assumption of a bimodal distribution [36] for the available channel balance (or channel liquidity) with density function

$$P(x) \sim e^{-\frac{x}{s}} + e^{\frac{x - \text{cap}_e}{s}}.$$

Here, s is a liquidity broadening scale that describes how quickly the bimodal distribution drops off from the extreme balance states of $x = 0$ and $x = \text{cap}_e$, respectively. A small value of s , relative to channel capacities, represents a strongly bimodal channel balance distribution. In contrast, a large value of s indicates that the channel balances are more uniformly distributed.

Following this assumption, an unconditional probability estimate for P_e can be derived without requiring prior knowledge, based solely on the overall channel liquidity distribution. A conditional probability estimate, on the other hand, can be obtained based on historical payment attempts, considering the previous successes and failures for a specific channel across multiple attempts. LND’s *Bimodal* mode follows this approach to calculate the channel success probability, where the knowledge of previous payment attempts’ successes and failures decays over time. We explain the implementation in Section VI-A.

D. Attempt Cost/Failure Cost, Hop Cost

These costs are similar to the fee described above. Unlike fees, these costs do not add to the payment amount and are referred to as virtual costs. They consist of two components: fixed (constant) virtual cost and proportional virtual cost.

A tunable virtual cost c^i , representing the cost of a failed payment attempt [10], can be multiplied to the edge-specific success probability term as introduced in Section IV-C2 to balance the trade-off between maximizing success probability and minimizing fees. It is important to choose this cost wisely, as it ensures payment success through a previously successful path, rather than attempting an untested but potentially less expensive route.

This virtual cost is called *attempt cost* in LND, where it is multiplied to the path success probability as shown in (4), and is referred to as *failure cost* in Eclair, where it is multiplied to the channel success probability.

Pathfinding can also incorporate a virtual cost as one of the weight terms a_e^i in (2) to optimize the path length. This virtual cost, called *hop cost*, is used in Eclair.

E. Channel Age

Each payment channel e has been funded by a certain funding transaction, which had been included in a specific Bitcoin blockchain block. Thus, the *age* of a channel is publicly readily available by computing the difference of the

block height of the funding transaction and the current block height. Within pathfinding, the channel age can potentially give an indication on the reliability of the channel for the purpose of payment routing, as it can be argued that older channels are more likely to be suitable for payment routing purposes, as non-performing channels would have been closed by either of the two nodes over a long period of time.

The channel age is currently used as a part of the channel weight definition in Eclair, cf. Section VI-D.

F. HTLC Minimum

A relevant channel-specific parameter for Lightning pathfinding, which is communicated by LN nodes via gossip, is the *HTLC minimum* parameter HtlcMin_e or `htlc_minimum_msat`, the minimal payment amount amt_e that will be forwarded in a hashed timelock contract (HTLC) routed by the outgoing node of channel e [24], [6, Chapter 10]. If the payment amount fails to meet the HTLC minimum of a channel, the sender might need to consider an alternative channel or pay an additional amount to route through the same channel. Consequently, in pathfinding, the sender aims not only to minimize fees associated with routing the payment but also to minimize the extra amount needed to meet the HTLC minimums. LDK uses the HTLC minimum in its weight function to penalize a channel with high HTLC minimum relative to its fee. Another way to avoid any payment failures due to not exceeding the HTLC minimum is to exclude channels with HTLC minimum above the intended payment amount entirely from the LN graph G for the purpose of pathfinding.

G. HTLC Maximum

A complimentary, but different role plays the *HTLC maximum* parameter HtlcMax_e or `htlc_maximum_msat`, which indicates an upper bound on the payment amount that an outgoing node in a channel is willing to forward [24], [6, Chapter 10]. In most channels of the current LN graph, this parameter is chosen to coincide with the capacity cap_e [37]. If HtlcMax_e is lower than cap_e , the channel can be further removed from the pathfinding graph G if the target payment amount exceeds its value. To the best of our knowledge, only LDK uses HTLC maximum information in its weight function by penalizing channels with HtlcMax_e larger than half of the channel capacity, with the intention to penalize channel probing.

On the other hand, it could be reasonable to not penalize, but *prioritize* channels with a HtlcMax_e setting significantly smaller than their capacity, as this setting could serve as a *valve* which regulates the flow payments to induce a better (e.g., more uniform) liquidity distribution within the channel, as pointed out in [37]. However, we are not aware of any LN node pathfinding modules that take this point of view into account via their weight functions so far. The difference between the opposite HTLC maximums $\text{HtlcMax}_{(u,v)}$ and $\text{HtlcMax}_{(v,u)}$ could also be taken into account as this might induce a change in the liquidity distribution over time [37].

V. PATHFINDING ALGORITHMS

In this section, we discuss variants of shortest path algorithms used in LN clients, specific constraints applied during the path selection, resulting implications on the problem complexity class and the optimality of respective solution paths.

A. Shortest Path Algorithms for Additive Costs

It is folklore in the Lightning Network developer community [6, Chapter 12] that the single-path pathfinding problem can simply and efficiently be solved by using Dijkstra’s algorithm [38], which has a worst-case runtime complexity of $O((|E| + |V|) \log(|V|))$ if its priority queue is implemented as a binary heap [31], [39], where $|E|$ is the number of channels and $|V|$ is the number of nodes in the Lightning Network graph. This makes Dijkstra’s algorithm (presented in Algorithm 1) a good choice if applicable, even in the presence of significant future growth of the Lightning Network.³

However, as we see below, some nuance is required, as not all costs defined by LN clients enable such an algorithm to find a path p that minimizes the cost over all eligible paths, and as additional constraints are typically imposed.

Given the Lightning Network graph $G = (V, E)$, many LN clients use Dijkstra’s algorithm $\text{DIJKSTRA}(G, \text{weight}_a, s)$ (Algorithm 1), to find the *cheapest* path from source $s \in V$ node (which is, technically, chosen to be the *recipient* node r of a Lightning payment) to all nodes $u \in V$ in the network (and in particular, to the *sender* of the LN payment) with respect to an additive total path cost $c(p)$ as in (1), where $\text{weight}_a : E \rightarrow \mathbb{R}_{\geq 0}$ is a non-negative channel-specific weight function. On a high level, within the algorithms, distances and predecessors for each vertex $u \in V$ are first initialized. A set S of vertices, whose final shortest-path weights from s have been determined, is maintained. Q is a min-priority queue of vertices, keyed by the total path weight $c_a(p)$ as defined in (1). Each vertex $u \in V$ is inserted into the priority queue Q , with its priority determined by its initial distance. While there exist vertices in Q to process, the vertex u with the smallest distance estimate $u.c_a(p)$ is extracted from Q and the shortest path to u is considered final and added to S . For each neighbor v of the vertex u , the algorithm attempts to relax the edge (u, v) , i.e., the algorithm checks whether the current best-known distance to v , $v.c_a(p)$, can be improved by traversing via the edge (u, v) . If the distance dist_a via u , $u.c_a(p) + \text{weight}_a(u, v)$, provides a shorter path to v , then the predecessor of v can be updated to u and the distance to v can be updated in Q , such that $v.c_a(p) = u.c_a(p) + \text{weight}_a(u, v)$.

It can be shown that $\text{DIJKSTRA}(G, \text{weight}_a, s)$ terminates such that the cheapest path to s from each node u in the graph, with respect to the additive path cost

$$c_a(p) = \sum_{e \in p} \text{weight}_a(e) \quad (7)$$

is implicitly found.

³The LN snapshot from 2022 we used [40] in our simulations has $|E| = 2 \cdot 57,773$ directed channels, cf. Section VII.

However, within LN clients, apart from the total path cost $c_a(p)$ of a path p , pathfinding is subject to certain (one or more) *side constraints* that can be expressed as

$$x(p) := \sum_{e \in p} y_e \leq \alpha \quad (8)$$

where x defines the constraint function with non-negative y_e , $e \in E$ and $\alpha \geq 0$ an upper bound. The constraints used by LN clients are related to the design elements explored in Section IV and try to impose certain payment path properties that are considered desirable, such as a maximum total fee (which, if exceeded by the path fee, makes a path non-desirable by the user) or a minimum path success probability. We summarize existing side constraints used by different LN clients during pathfinding in Table I.

In practice, the adherence of paths to a constraint (8) is achieved by adding the colored lines in Algorithm 1, which makes sure that any constructed path does not violate (8). In particular, Algorithm 1 only updates the the distance of v in Q and the predecessor of v for a neighbor node v of u if the new constraint value $\text{cstval} = u.x(p) + y(u, v)$ does not exceed the bound α , i.e., if $\text{cstval} \leq \alpha$. While the colored modification in Algorithm 1 only implies the adherence to one constraint (8), this modification can be analogously extended to multiple constraints $x_1(p) \leq \alpha_1, \dots, x_m(p) \leq \alpha_m$.

Algorithm 1 Dijkstra’s Algorithm [38] (with **colored** modification if to impose constraint $x(p) \leq \alpha$) for cost (7)

```

DIJKSTRA( $G, \text{weight}_a, y, \alpha$ ,  $s$ )
for each vertex  $u \in V$  do
     $u.c_a(p) \leftarrow +\infty$ 
     $u.\text{prev} \leftarrow \text{UNDEFINED}$ 
end for
 $S \leftarrow \emptyset$ 
 $Q \leftarrow \emptyset$ 
 $s.c_a(p) \leftarrow 0$ 
 $s.x(p) \leftarrow 0$ 
for each vertex  $u \in V$  do
    INSERT( $Q, u$ )
end for
while  $Q \neq \emptyset$  do
     $u \leftarrow \text{EXTRACT-MIN}(Q)$ 
     $S \leftarrow S \cup \{u\}$ 
    for each vertex  $v \in \text{Adj}[u]$  do
         $\text{dist}_a \leftarrow u.c_a(p) + \text{weight}_a(u, v)$ 
         $\text{cstval} \leftarrow u.x(p) + y(u, v)$ 
        if  $\text{dist}_a < v.c_a(p)$  &  $\text{cstval} \leq \alpha$  then
             $v.\text{prev} \leftarrow u$ 
             $v.c_a(p) \leftarrow \text{dist}_a$ 
             $v.x(p) \leftarrow \text{cstval}$ 
            DECREASE-KEY( $Q, v, \text{dist}_a$ )
        end if
    end for
end while

```

TABLE I: Side constraints used by LN clients during pathfinding

Constraint		LN Client
Timelock	$\sum_{e \in p} \Delta_e^{\text{CLTV}} \leq \text{Max_CLTV_Limit}$	LND, LDK
Probability	$-\sum_{e \in p} \log(P_e) \leq -\log(\text{Min_Prob_Limit})$	LND
Fee	$\sum_{e \in p} \text{fee}_e \leq \text{Max_Fee_Limit}$	LND, LDK
Path Length	$\sum_{e \in p} 1 \leq \text{Max_PathLength_Limit}$	LDK, CLN*, Eclair*

* Constraints are validated after pathfinding.

The constraint-adhering version DIJKSTRA($G, \text{weight}_a, y, \text{alpha}, s$) of Algorithm 1 can be interpreted as a *greedy algorithm* for solving the so-called *constrained shortest-path problem* (with respect to cost (7) and constraint (8)), a problem class that has been studied by a considerable body of literature [34, Chapter 16], [41, Section 8.4], [42]–[45].

While the conventional shortest path problem can be solved, e.g., by Algorithm 1 in a time that is essentially *linear* in $|E|$ as mentioned above, the constrained shortest-path problem is known to be \mathcal{NP} -complete, [34, Appendix B.4], [41, Section 8.4], which implies that, unless $\mathcal{P} = \mathcal{NP}$, no polynomial-time algorithm exists that can solve the constrained shortest-path problem for all problem instances. Thus, the output of DIJKSTRA($G, \text{weight}_a, y, \text{alpha}, s$) will not be able to optimally solve the problem it is designed for solving in general.

B. Shortest Path Algorithms for Additive+Multiplicative Costs

We discussed in Section IV-C that path cost modelling used in the LND LN client implementation amounts to a additive-plus-multiplicative cost function $c(p)$, which was defined in (5). In order to find paths p that minimize such a cost $c(p)$, LND uses a modified Dijkstra-style algorithm, which we outline in Algorithm 2. In particular, compared to Algorithm 1, the priority queue is keyed based on the additive-plus-multiplicative cost $c(p)$ instead of on a purely additive cost (7), and the algorithm MODDIJKSTRA($G, \text{weight}_a, \text{weight}_m, c_{\text{attempt}}, s$) takes as additional input a multiplicative weight function $\text{weight}_m : E \rightarrow \mathbb{R}_{\geq 1}$ with outputs larger than or equal 1, and an initial cost term factor c_{attempt} .

Similar to Algorithm 1, after initialization, each neighboring vertex v of $u \in Q$ is processed. During the relaxation of the edge (u, v) , the algorithm computes the total additive weight dist_a as $u.c_a(p) + \text{weight}_a(u, v)$ and the total multiplicative weight dist_m as $u.c_m(p) \cdot \text{weight}_m(u, v)$. The predecessor of v is updated to u and the additive-plus-multiplicative distance $\text{dist}_a + \text{dist}_m$ is updated for v in Q , provided the distance $\text{dist}_a + \text{dist}_m$, is greater than the previous distance to v , $v.c_a(p) + v.c_m(p)$.

It turns out that, even without the imposition of any side constraints (8) (no colored modification in Algorithm 2), Algorithm 2 is not guaranteed to find the optimal path cannot always be guaranteed due the multiplicative weight used in $c(p)$ of (5).

To illustrate the suboptimality of MODDIJKSTRA($G, \text{weight}_a, \text{weight}_m, c_{\text{attempt}}, s$), consider a directed

Algorithm 2 Dijkstra-Style Algorithm Modified for Additive+Multiplicative Cost (5) as used in LND (with **colored** modification if to impose constraint $x(p) \leq \text{alpha}$)

```

MODDIJKSTRA( $G, \text{weight}_a, \text{weight}_m, c_{\text{attempt}}, y, \text{alpha}, s$ )
for each vertex  $u \in V$  do
     $u.c_a(p) \leftarrow +\infty$ 
     $u.c_m(p) \leftarrow 0$ 
     $u.\text{prev} \leftarrow \text{UNDEFINED}$ 
end for
 $S \leftarrow \emptyset$ 
 $Q \leftarrow \emptyset$ 
 $s.c_a(p) \leftarrow 0$ 
 $s.c_m(p) \leftarrow c_{\text{attempt}}$ 
 $s.x(p) \leftarrow 0$ 
for each vertex  $u \in V$  do
    INSERT( $Q, u$ )
end for
while  $Q \neq \emptyset$  do
     $u \leftarrow \text{EXTRACT-MIN}(Q)$ 
     $S \leftarrow S \cup \{u\}$ 
    for each vertex  $v \in \text{Adj}[u]$  do
         $\text{dist}_a \leftarrow u.c_a(p) + \text{weight}_a(u, v)$ 
         $\text{dist}_m \leftarrow u.c_m(p) \cdot \text{weight}_m(u, v)$ 
         $\text{cstval} \leftarrow u.x(p) + y(u, v)$ 
        if  $(\text{dist}_a + \text{dist}_m) < (v.c_a(p) + v.c_m(p))$ 
        &  $\text{cstval} \leq \text{alpha}$  then
             $v.\text{prev} \leftarrow u$ 
             $v.c_a(p) \leftarrow \text{dist}_a$ 
             $v.c_m(p) \leftarrow \text{dist}_m$ 
             $v.x(p) \leftarrow \text{cstval}$ 
            DECREASE-KEY( $Q, v, \text{dist}_a + \text{dist}_m$ )
        end if
    end for
end while
    
```

graph $G = (V, E)$ as shown in Figure 1. This graph consists of six nodes $V = \{r, s, h, i, j, k\}$ and seven edges $E = \{(s, h), (s, k), (h, i), (h, j), (k, j), (i, r), (j, r)\}$. Each edge $e \in E$ comprises of an additive weight $\text{weight}_a(e)$ and a multiplicative weight $\text{weight}_m(e)$, denoted with subscript a and with subscript m in Figure 1, respectively. To calculate the total path cost, we use (5), where the virtual attempt cost c_{attempt} is taken as 1. For simplicity, we do not impose side constraints such as (8) in this example—additional side

constraints make the problem even harder, and suboptimality is easier to show.

To find a path from source s to recipient r using Algorithm 2, the algorithm first initializes the additive weight $c_a(p)$ and the multiplicative weight $c_m(p)$ for each vertex to ∞ and 0, respectively, then set S , and the priority queue Q . Starting from source s , we relax the adjacent nodes, h and k , of s . From s , the distance to h is calculated as $h.c_a(p) + h.c_m(p) = 4 + 1 = 5$. Similarly, $k.c_a(p) + k.c_m(p) = 1 + 2 = 3$. The priority queue is keyed based on the distances for subsequent relaxations as $Q = \{(k, 3), (h, 5)\}$. Now, k is removed from the priority queue and its neighbor j is relaxed. The distance to j is calculated as $1 + 1 + 2 \cdot 2 = 6$. Since the distance to j from s , via k , is greater than the distance to h from s , node j will be added to the end of Q as $\{(h, 5), (j, 6)\}$. As a next step, we therefore remove h from the queue, and the distance to its neighbor i is obtained as $4 + 2 + 2 = 8$, and we get the distance to j as $4 + 2 + 1 = 7$. However, the already known distance to j via k is 6 which is shorter than the distance via h . Consequently, the distance to j in Q will not be updated based on the distance via h . With $Q = \{(j, 6), (i, 8)\}$, node j will be removed from the queue, and the edge to its neighbor r is relaxed, giving the distance to r as $1 + 1 + 2 \cdot 2 \cdot 5 = 22$. Then, node i will be removed from the queue and its edge to r is relaxed, yielding the distance to r as $4 + 2 + 4 + 1 \cdot 2 \cdot 2 = 14$. Hence, the algorithm terminates and returns the path $s \rightarrow h \rightarrow i \rightarrow r$ with the cost of $r.c_a(p) + r.c_m(p) = 14$.

However, this is not the optimal path, as the cost of the path $s \rightarrow h \rightarrow j \rightarrow r$ is $4 + 2 + 1 \cdot 1 \cdot 5 = 11$, which is cheaper than the path returned by Algorithm 2. The algorithm ignores this path during relaxation, as illustrated, due to the nature of the additive-plus-multiplicative cost as in (5), which leads the algorithm to greedily select the predecessor based on the current weight, thereby excluding potentially less expensive routes. Via this counterexample, we conclude that, while the algorithm might often behave reasonably, the modified Dijkstra-style algorithm $\text{MODDIJKSTRA}(G, \text{weight}_a, \text{weight}_m, c_{\text{attempt}}, s)$ used in LND cannot *guarantee* to return an optimal path with respect to its modelled cost function (5).

While it is possible to tune the value of c_{attempt} to give more weight to the multiplicative weight $c_m(p)$ in (5) to fix the behavior for this example, a counterexample for optimality can be found for any choice of c_{attempt} .

C. K -Shortest Path Algorithms

Beyond Dijkstra-type algorithms to find a single shortest path between sender and receiver nodes of a payment with respect to a fixed path cost function as presented in Algorithm 1 and Algorithm 2, there are also LN clients that return a *selection* of candidate paths during pathfinding.

For this purpose, in particular, Yen’s K -shortest path algorithm [46] is used. This algorithm uses a shortest path algorithm (such as Algorithm 1) as a subroutine, but returns a list of K “best” paths with respect to the imposed cost

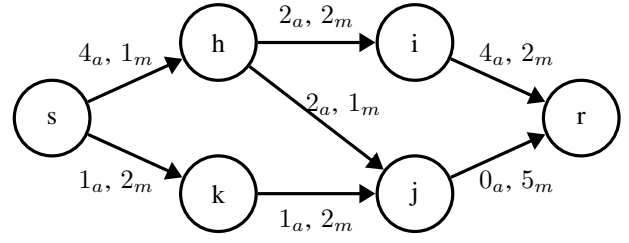


Fig. 1: Counterexample graph G for suboptimality of Algorithm 2 for pathfinding with respect to additive-plus-multiplicative cost (5).

function. If Dijkstra’s algorithm is used as a subroutine, and if no constraints (8) are imposed, the worst-case time complexity of the algorithm is $O(K|V|(|E| + |V|) \log(|V|))$ (for Dijkstra implemented with binary heap) [47, Section 6.3]. This complexity might limit the scalability of the approach in case of further growth of the Lightning Network. Yen’s K -shortest path algorithm is currently used only in the Eclair LN client.

VI. IMPLEMENTATION OF PATHFINDING IN LIGHTNING NODE CLIENTS

In this section, we detail the single-path pathfinding strategies employed by the four popular Lightning node clients LND, CLN, LDK, and Eclair, with a particular focus on a breakdown of the defined cost functions/ edge weights, including relevant constants and default values. Each of these Lightning node clients finds a payment path using one of the algorithms discussed in Section V. LND utilizes the modified Dijkstra-style algorithm Algorithm 2, CLN, and LDK use Algorithm 1, whereas Eclair utilizes Yen’s K -shortest path algorithm. Each of them uses significantly different weight functions $\text{weight} : E \rightarrow \mathbb{R}_{\geq 0}$ with different trade-offs. To accurately compute the fee fee_e associated with using a channel between nodes, all these clients perform the path search backwards from the receiver node to the source node.

A. LND

In LND, the weight function considers various design elements mentioned in Section IV, including the payment amount and fee for using the channel e as well as the CLTV delta Δ_e^{CLTV} and a penalty term related to the estimated success probability. Specifically, the weight function is defined as

$$\text{weight}(e) = \text{fee}_e + \text{amt}_e \cdot \Delta_e^{\text{CLTV}} \cdot \text{riskfactor} + \frac{\text{penalty}_e}{P_p}, \quad (9)$$

In this equation, fee_e and Δ_e^{CLTV} are specific to the channel and are obtained through the channel update messages [48] within the network. In LND, the influence of the Δ_e^{CLTV} is controlled by scaling it using the riskfactor, which defaults to a value of $15 \cdot 10^{-9}$.

$$\text{penalty}_e = \text{attemptcost}_e \cdot \frac{1}{0.5 - \frac{0.9 \cdot \text{timepref}}{2}} - 1. \quad (10)$$

In the above equation, timepref is the time preference for the payment. It is set to -1 to prioritize optimizing for fees only, set to 1 to prioritize optimizing for reliability only, or set to a value in between for a balanced approach. By default, its value is 0.

$$\begin{aligned} \text{attemptcost}_e &= \text{BaseAttemptCost} \\ &+ \text{amt}_e \cdot \text{AttemptCostRate}. \end{aligned} \quad (11)$$

The weight function also incorporates the design element *attempt cost* (Section IV-D). This is a predetermined virtual cost that signifies the cost of a failed payment attempt, denoted as attemptcost_e . This serves as a parameter in the weight function to balance the consideration of potentially better routes against the success probability of the payment. The default values of BaseAttemptCost and AttemptCostRate are 100 msat and 1000 msat respectively.

Additionally, LND takes into account the success probability of the path P_p as one of its weight function design elements, given by,

$$P_p = \prod_{e \in p} P_e \quad (12)$$

where $p = (e_1, \dots, e_{\text{length}(p)})$ is the path.

It keeps records of past failed payment attempts within a channel, allowing for the tracking of the time elapsed since the last failure. This information is used in calculating success probabilities, underscoring LND's emphasis on prioritizing reliable routing paths. LND uses two distinct methods for calculating the channel-wise success probability P_e of a channel forwarding a payment: Apriori and Bimodal.

In Apriori, the success probability is influenced by the weight of the last failure. Initially, when a failure occurs, the success probability drops to zero. However, over time, based on the defined PenaltyHalfLife period, the success probability gradually recovers to its node probability (nodeProb_e) via the formula

$$P_e = \text{nodeProb}_e \cdot \left(1 - \frac{1}{2^{\frac{\text{timeSinceLastFailure}_e}{\text{PenaltyHalfLife}}}}\right). \quad (13)$$

In the above equation, nodeProb_e is given by,

$$\text{nodeProb}_e = P_{\text{apriori}} \cdot \left(1 - \frac{0.5}{1 + e^{\frac{c_o \cdot \text{cap}_e - \text{amt}_e}{s_o \cdot \text{cap}_e}}}\right). \quad (14)$$

The assumption made by LND, in this case, is that each hop has P_{apriori} (base success likelihood) of 0.6. The values of c_o and s_o in (14), which represent the fraction of channel capacity cap_e at which probability reweighing becomes noticeable and the rate at which probability adjustments occur [33], respectively, are set to 0.9999 and 0.025. The preset PenaltyHalfLife is 1 hour.

In Bimodal estimation of success probability, LND assumes a bimodal distribution $P(x) \sim e^{-\frac{x}{s}} + e^{-\frac{x - \text{cap}_e}{s}}$ as explained

in Section IV-C2. The liquidity broadening scale s gets the default value of $3 \cdot 10^8$ sats.

In this context, the success probability for a payment amount is determined by integrating over the prior distribution, $P(x)$. However, if information regarding previous success and failure amounts is available, the prior distribution $P(x)$ is being adjusted. The posterior distribution is then derived by re-normalizing the prior distribution such that

$$P_e = \frac{\int_{\text{amt}_e}^{\text{fa}_e} P(x) dx}{\int_{\text{sa}_e}^{\text{fa}_e} P(x) dx}. \quad (15)$$

Upon solving the integral we get the following equation for channel-wise success probability,

$$P_e = \frac{e^{\frac{(\text{fa}_e - \text{cap}_e)}{s}} - e^{-\frac{\text{fa}_e}{s}} - e^{\frac{(\text{amt}_e - \text{cap}_e)}{s}} + e^{-\frac{\text{amt}_e}{s}}}{e^{\frac{(\text{fa}_e - \text{cap}_e)}{s}} - e^{-\frac{\text{fa}_e}{s}} - e^{\frac{(\text{sa}_e - \text{cap}_e)}{s}} + e^{-\frac{\text{sa}_e}{s}}} \quad (16)$$

where sa_e and fa_e represent the unsettled success and failure amounts, respectively and cap_e is the channel capacity.

From (16), it can be noted that the bimodal estimator provides insights about sending amounts based on previous success and failure amounts, unlike the apriori estimator (13) which does not provide such insights.

The weight function (9) used by LND is founded on the principle of assessing channels with high reliability, characterized by low fees and short timelocks. This rationale is reflected in the weight function's consideration of fees, timelock, and success probability.

B. CLN

Design elements considered in the weight function of CLN are amount, fee, timelock and riskfactor, leading to the weight function

$$\begin{aligned} \text{weight}(e) &= \left(\text{fee}_e + \frac{\text{amt}_e \cdot \Delta_e^{\text{CLTV}} \cdot \text{riskfactor}}{\text{BlockPerYear} \cdot 100} + 1 \right) \\ &\cdot (\text{capacityBias}_e + 1) \end{aligned} \quad (17)$$

for the channel e . Similar to its application in LND as observed in (9) with Δ_e^{CLTV} , the riskfactor is used here in conjunction with Δ_e^{CLTV} to regulate its impact. The default value for the riskfactor is 10. Essentially, in (17), the percentage of yearly expense incurred by funds trapped within the channel is considered. With 52,596 blocks per year, the yearly cost per block equates to the $\frac{1}{5,259,600}$.

Additionally, CLN introduces capacityBias_e to penalize channels where a substantial portion of the channel's total capacity is being utilised. The formulation of capacityBias_e is based on modeling the channel-wise success probability under the assumption of uniform liquidity distribution mentioned in [14]. It is given by,

$$\text{capacityBias}_e = -\log \left(\frac{\text{cap}_e + 1 - \text{amt}_e}{\text{cap}_e + 1} \right). \quad (18)$$

(18) is similar to (6) with $P_e = \frac{\text{cap}_e + 1 - \text{amt}_e}{\text{cap}_e + 1}$.

Analysis of Equation (17) illustrates a notable emphasis on Δ_e^{CLTV} through the selection of higher value for the riskfactor .

Consequently, CLN is inclined to favor paths characterized by lower timelock.

C. LDK

LDK incorporates design elements such as fees and HTLC minimum into its weight function, along with penalty. The weight function for using the channel e in LDK is as given below,

$$\text{weight}(e) = \max(\text{fee}_e, \text{pathHtlcMin}_e) + \text{penalty}_e. \quad (19)$$

In routing, payments must meet the minimum HTLC limit set by each channel that is used as described in Section IV. Therefore, to utilize the channel by meeting the HTLC minimum, the payment source might have to pay an additional amount along with the actual payment amount. This additional amount is denoted as pathHtlcMin_e . HtlcMin_e in the equation below is obtained from the channel update message [48].

$$\begin{aligned} \text{pathHtlcMin}_e &= \text{HtlcMin}_e \cdot (1 + \text{feeRate}_e) \\ &+ \text{BaseFee}_e. \end{aligned} \quad (20)$$

penalty_e in the channel weight is the sum of base penalty, anti probing penalty and total liquidity penalty, expressed as:

$$\begin{aligned} \text{penalty}_e &= \text{basePenalty}_e + \text{antiProbingPenalty}_e \\ &+ \text{liquidityPenalty}_e + \text{historicPenalty}_e. \end{aligned} \quad (21)$$

Base penalty comprises of a fixed penalty penaltyBase , which is applied to each channel has default value 500 msat, and baseMultiplier , which is used with amount in the channel, with default value 8,192 msat. The purpose of using baseMultiplier with amount is to avoid having fees dominate the channel weight for large amount.

$$\text{basePenalty}_e = \text{penaltyBase} + \frac{\text{baseMultiplier} \cdot \text{amt}_e}{2^{30}}. \quad (22)$$

The anti-probing penalty in (21) is set to 250 msat is applied if a channel's HTLC maximum (HtlcMax_e) is equal to or greater than half of the channel's capacity cap_e , and set to 0 otherwise, in order to prefer channels with smaller HtlcMax_e , i.e.,

$$\text{antiProbingPenalty}_e = \begin{cases} 250, & \text{if } \text{HtlcMax}_e \geq \frac{\text{cap}_e}{2}, \\ 0, & \text{otherwise.} \end{cases} \quad (23)$$

In $\text{liquidityPenalty}_e$ calculation, a multiplier LM is used, with the negative logarithm of the channel-wise success probability P_e for a payment. The preset value of this multiplier is 30,000 msat. Additionally, an amtMultiplier_e is used in $\text{liquidityPenalty}_e$ calculation. The penalty is influenced by the latest estimate of the liquidity in the channel.

$$\begin{aligned} \text{liquidityPenalty}_e &= -\log_{10}(P_e) \\ &\cdot (\text{LM} + \text{amtMultiplier}_e). \end{aligned} \quad (24)$$

historicPenalty_e is similar to $\text{liquidityPenalty}_e$. However, in this case, instead of solely relying on the latest estimate of the liquidity available in the channel, the calculation of the success probability is based on the historical estimated

liquidity available in the channel. A multiplier HM is also utilized alongside the negative logarithm of the channel's success probability P_e for the payment. This calculation is based on the historical estimates of the channel's available liquidity. It takes the default value 10,000 msat.

$$\begin{aligned} \text{historicPenalty}_e &= -\log_{10}(P_e) \\ &\cdot (\text{HM} + \text{amtMultiplier}_e). \end{aligned} \quad (25)$$

amtMultiplier_e in Equation (24) and Equation (25) is given by,

$$\text{amtMultiplier}_e = \frac{\text{Multiplier} \cdot \text{amt}_e}{2^{20}}. \quad (26)$$

In the above equation, Multiplier is $\text{liquidityPenaltyMultiplier}$ set to 192 msat and $\text{historicPenaltyMultiplier}$ set to 64 msat in the case of $\text{liquidityPenalty}_e$ and historicPenalty_e , respectively.

A channel's success probability P_e is calculated using upper and lower liquidity bounds UB_e and LB_e that are determined using the past unsuccessful and successful payments based on the formula

$$P_e = \frac{\text{UB}_e - \text{amt}_e}{\text{UB}_e - \text{LB}_e}. \quad (27)$$

This calculation, similar to (18), also based on modeling the success probability under uniform liquidity distribution assumption as described in [14].

As the weight function of LDK (19) considers the maximum value between fee and HTLC minimum, selecting a channel with the minimum fee may not always be possible. In scenarios where two paths have the same fees but different HTLC minimums, the path with higher HTLC minimum may be chosen. This can compel the sender to pay additional fees to meet the HTLC minimum, especially when the payment amount is small, potentially resulting in higher overall fees for the sender.

D. Eclair

In Eclair, weight computation involves three distinct cases, which are discussed in detail below.

1) *Case 1: Heuristics ratios:* In this case, weight of an edge is based on the design elements including fee, channel age, CLTV delta, capacity and a virtual hop cost, such that

$$\text{weight}(e) = (\text{fee}_e + \text{HopCost}_e) \cdot \text{factor}_e \quad (28)$$

where factor_e is given by,

$$\begin{aligned} \text{factor}_e &= \text{basefactor} + (n_{\text{cltv}_e} \cdot \text{CLTVfactor}) \\ &+ (n_{\text{age}_e} \cdot \text{agefactor}) + ((1 - n_{\text{cap}_e}) \cdot \text{capfactor}). \end{aligned} \quad (29)$$

factor_e includes heuristics ratios and the normalized values. Eclair utilizes default ratios 0.35, 0, 0.5 and 0.15 for agefactor , basefactor , capfactor and CLTVfactor respectively. Eclair computes the normalized values of $\Delta_e^{\text{CLTV}}(n_{\text{cltv}_e})$, channel age (n_{age_e}) and capacity (n_{cap_e}) as given in (30). The block height of the channel's funding transaction is taken as the channel age.

The calculation for the normalized value $n_D(v)$ of a real number v within the range D is as follows:

$$n_D(v) = 0.00001 + 0.99998 \cdot \frac{\min(\max(\min D, v), \max D) - \min D}{\max D - \min D} \quad (30)$$

where $\min D$ and $\max D$ represent the minimum and maximum values in the range D , respectively.

2) *Case 2: Heuristics constants (without logarithm)*: In this case, the weight of an edge takes into account the risk cost, a virtual failure cost, and channel-wise success probability, alongside the fees and hop cost for the channel e :

$$\text{weight}(e) = \text{fee}_e + \text{HopCost}_e + \text{RiskCost}_e + \left(\frac{\text{FailureCost}_e}{P_e} \right). \quad (31)$$

3) *Case 3: Heuristics constants (with logarithm)*: This case is similar to case 2, but here, the weight function incorporates the logarithm of success probability, such that

$$\text{weight}(e) = \text{fee}_e + \text{HopCost}_e + \text{RiskCost}_e - \text{FailureCost}_e \cdot \log(P_e). \quad (32)$$

In cases 2 and 3, success probability is determined by computing the ratio of the amount to the capacity, as given below,

$$P_e = 1 - \frac{\text{amt}_e}{\text{cap}_e}. \quad (33)$$

In routing, as mentioned in Section IV, there is a constant risk of funds being locked in HTLC. This risk is represented by the heuristic constant in Eclair, denoted as `lockedFundsRisk`, with a preset value of 10^{-8} . Therefore, RiskCost_e is calculated to manage the influence of timelock constraints.

$$\text{RiskCost}_e = \text{amt}_e \cdot \Delta_e^{\text{CLTV}} \cdot \text{lockedFundsRisk}. \quad (34)$$

Failure cost represents a virtual cost associated with failed payment attempt, similar to the use of attempt cost in LND (11).

$$\text{FailureCost}_e = \text{BaseFailureCost} + \text{amt}_e \cdot \text{FailureCostRate} \quad (35)$$

where `BaseFailureCost` and `FailureCostRate` are given with default values 2000 msat and 500 msat respectively.

$$\text{HopCost}_e = \text{BaseHopCost} + \text{amt}_e \cdot \text{HopCostRate}. \quad (36)$$

The default values of `BaseHopCost` and `HopCostRate` are both zero. Fine-tuning HopCost_e can be considered to optimize for different performance metrics.

The fees associated with per-hop charges and failed attempts are not actually spent. They function as incentives to favor shorter paths or routes with greater probability of success.

In this section, we present the simulation model designed to evaluate the empirical performance of four LN clients (LND v0.17.4-beta, CLN v24.02.1, LDK v0.0.120, and Eclair v0.10.0), including their variations outlined in Section VI. We also discuss our experiment methodology, results, and observations based on various evaluation metrics.

Our simulation model is developed using Python 3.11 for all experiments. The source code is available on GitHub at: <https://github.com/sindurasaraswathi/LN-PathFinding>.

The Lightning Network graph is constructed from the dataset [40], and all graph-related operations are performed using the Networkx library [49]. The utilized Lightning Network snapshot [40] comprises 13,129 nodes and 57,773 channels, providing channel-specific information such as short channel ID, channel ID, capacity, base fee, proportional fee, minimum and maximum HTLC, and CLTV delta.

All relevant information required for pathfinding and used in weight functions as design elements is included as attributes of the channel in the generated graph. Channel age is extracted using the short channel ID. We constructed two LN graphs. The first graph is built by uniformly choosing channel balances between zero and the channel capacity. The second graph is constructed by sampling channel balances from a bimodal distribution $P(x) \sim e^{-\frac{x}{s}} + e^{\frac{x-\text{cap}_e}{s}}$, where s is selected as a fixed fraction of the channel capacity, specifically $s = \frac{\text{cap}_e}{10}$. We refer to the first and second graphs as the uniform distribution graph and the bimodal distribution graph, respectively, throughout this section.

In general, the Lightning Network comprises of nodes with varying levels of connectivity, determined by factors such as capacity and the number of channels. For instance, as mentioned in [6], there are nodes operated by prominent merchants, which are typically well-funded and highly connected with numerous channels. Conversely, there are nodes with moderate connectivity, possessing adequate capacity and channels. Additionally, the network includes nodes that are poorly connected, lacking in channels and funds.

Understanding the routing behavior of nodes across these different connectivity levels is also crucial. Hence, we classify the nodes into well-connected, fairly connected, and poorly connected categories based on the total capacity across all channels originating from a node and the number of channels. Specifically, nodes with a total capacity greater than or equal to 10^6 sats and more than 5 channels are categorized as well-connected, those with a total capacity falling between 10^4 and 10^6 sats and more than 5 channels are classified as fairly connected, and nodes with 5 or fewer channels are designated as poorly connected, regardless of their total channel capacity. The statistics on node connectivity, including the number of nodes and channels, as well as the channel capacity for each node category, are presented in Table II.

We conducted several experiments to compare the empirical performance of the four Lightning clients and their variations. Initially, using the uniform distribution graph, simulations

TABLE II: Node connectivity statistics

Connectivity Level	Node count	Median channel count	Median capacity
Well-connected	3476	12	24616394
Fairly-connected	53	6	535000
Poorly-connected	9600	1	125000

were performed for 10,000 transactions, with source and receiver nodes randomly selected from all nodes in the graph. Transaction amounts were uniformly chosen between 1 and the minimum of the maximum values of all outgoing channel balances of the source node and all local incoming balances of the receiver node. By using this upper bound, we were able to select payment amounts that are practically feasible for the source node to send and for the receiver node to receive.

We used the *_dijkstra* method from the Networkx library to execute the Dijkstra’s algorithm for CLN and LDK, and adapted *_dijkstra* for LND as discussed in Section V, supplying the method with an appropriate weight function and side constraints. For finding Yen’s K shortest paths in the case of Eclair, we adapted the *shortest_simple_paths* method from the Networkx library. Upon determining a path for a given lightning variant and transaction, our model simulated the routing of the payment amount through the determined path. The routing was regarded a failure if no acceptable path could be found or if any of the intermediaries nodes had insufficient balances.

In our experiments, we studied and compared a total of seven variants of LN clients: LND1, LND2, CLN, LDK, Eclair_case1, Eclair_case2, and Eclair_case3. LND1 and LND2 represent the LND implementation with Apriori and Bimodal estimators, respectively, for channel-wise success probability calculation. Similarly, Eclair_case1, Eclair_case2, and Eclair_case3 denote three distinct cases of Eclair: heuristics ratios, heuristics constants (without logarithm) and heuristics constants (with logarithm), respectively, as discussed in Section VI.

We investigated the behavior of each variant of the LN clients across various transaction amount bins, spanning the range from 1 to 10^8 . From Figure 2, it is evident that LND2 exhibits the highest success rate and excels particularly with larger payment amounts. Conversely, LND1 demonstrates the lowest success rates in the mid-range amount bins. CLN’s success rate remains competitive for larger amounts, while LDK performs well by delivering the highest success rates for small and lower mid-range amounts; however, its success rate experiences a significant decline for larger amounts. Eclair_case1 and Eclair_case2 demonstrate similar performance levels, with higher success rates observed for larger payment amounts compared to LDK and CLN. Meanwhile Eclair_case3 exhibits higher success rates than Eclair_case1 and Eclair_case2 and its performance is closer to LND2, making it a competitive performer in terms of success rate.

While the success rate, or payment reliability, remains a crucial metric in pathfinding algorithm design, it is not the sole consideration. Factors such as the fee incurred, the

path length, and the total timelock or latency along the path also play significant roles. Consequently, we conducted a comparative analysis of LN client variants based on these metrics. The distribution of fee across transaction amount bins is illustrated in Figure 3. Additionally, the distribution of path lengths observed across routing client variants is represented in Figure 4.

Table IV presents a summary of metrics, encompassing fee, path length, and timelock, observed across routing clients. To ensure the robustness of our comparative analysis regarding these metrics, we exclusively considered transactions where routing succeeded in four or more routing client variants. In our analysis of the fee metric, we calculated the ratio of the fee to the transaction amount and determined the median across all transactions under consideration. Similarly, we computed the average path length and timelock across all transactions considered.

Regarding these metrics, as shown in Table IV, Eclair_case3 demonstrates effective performance in terms of fee along the path, providing the lowest fee ratio compared to other clients. LND2, in addition to achieving a high success rate, yields paths with lower fees but relatively longer path lengths. LND1, on the other hand, offers paths with significantly high fees but shorter path lengths and lower latency. Among the routing clients, LDK exhibits the highest fee ratio. However, for larger payment amounts, as can be seen in Figure 3d, LDK offers the lowest fee ratio compared to all other clients. CLN emerges as the top performer in terms of total timelock, offering paths with the lowest latency for routing payment amounts. Eclair_case1 and Eclair_case2 perform the best in terms of path length, while Eclair_case3 exhibits the highest path length and latency.

We conducted similar simulations on the bimodal distribution graph, to examine the performance of the LN clients when channel liquidity is predominantly concentrated on one side. As shown in Table V, LND2 yields the highest success rate across multiple amount bins, specifically for large payment amounts. While we used the default value ($3 \cdot 10^8$) for the liquidity broadening scale s in bimodal probability estimation (16), we also tested alternative values, including $\frac{\text{cap}_e}{10}$ — the same scale used during channel liquidity sampling. However, LND2 did not produce better results with these alternative values compared to the default. Similar to the uniform distribution case Table III, LDK performs better for low and lower mid-range amount bins compared to higher amount bins. However, Eclair_case1 and Eclair_case2 deliver competitive success rates and outperform Eclair_case3, unlike in the uniform distribution case. LND1 still demonstrates lower success rates, while CLN shows the lowest success rate

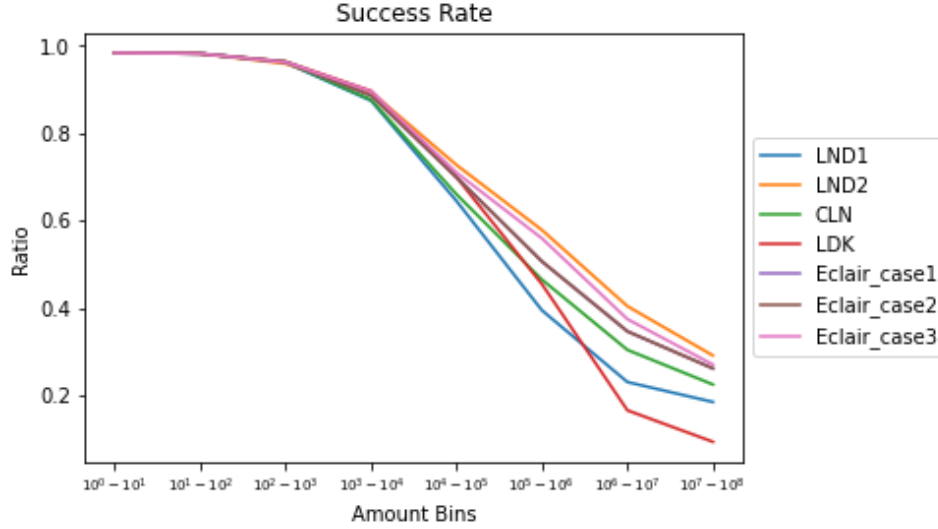


Fig. 2: Rate of success of different lightning clients across transaction amount bins

TABLE III: Success rates among Lightning Network clients across transaction amount ranges for uniform distribution graph

Amount Bins	LND1	LND2	CLN	LDK	Eclair_case1	Eclair_case2	Eclair_case3
$10^0 - 10^1$	98.414	98.414	98.414	98.414	98.414	98.414	98.414
$10^1 - 10^2$	98.226	98.226	98.226	98.226	98.226	98.226	98.226
$10^2 - 10^3$	96.157	95.917	96.317	96.397	96.317	96.317	96.237
$10^3 - 10^4$	87.440	89.440	87.680	89.680	88.640	88.640	89.600
$10^4 - 10^5$	64.480	72.720	66.000	69.920	69.920	69.920	70.960
$10^5 - 10^6$	39.440	57.840	46.480	45.440	50.640	50.640	55.920
$10^6 - 10^7$	23.040	40.400	30.400	16.560	34.640	34.640	37.440
$10^7 - 10^8$	18.480	29.120	22.480	9.360	26.160	26.160	27.040

TABLE IV: Comparison of fee ratio, path length, and timelock metrics across Lightning Network Clients for uniform distribution graph

Attribute	LND1	LND2	CLN	LDK	Eclair_case1	Eclair_case2	Eclair_case3
Fee	0.051%	0.016%	0.030%	0.070%	0.053%	0.053%	0.012%
Path Length	4.431	6.277	4.614	4.541	4.421	6.555	6.555
Timelock	195.499	258.426	187.738	200.857	196.053	196.053	270.158

TABLE V: Success rates among Lightning Network clients across transaction amount ranges for bimodal distribution graph

Amount Bins	LND1	LND2	CLN	LDK	Eclair_case1	Eclair_case2	Eclair_case3
$10^0 - 10^1$	97.871	97.950	97.792	97.792	97.792	97.792	97.871
$10^1 - 10^2$	96.429	96.104	96.347	96.429	96.266	96.266	96.023
$10^2 - 10^3$	92.560	92.560	92.400	92.880	92.640	92.640	93.120
$10^3 - 10^4$	71.840	73.040	72.560	73.600	72.640	72.640	72.800
$10^4 - 10^5$	44.960	50.480	44.240	50.160	49.040	49.040	48.880
$10^5 - 10^6$	24.080	33.280	24.160	25.360	29.680	29.680	29.680
$10^6 - 10^7$	16.560	18.720	16.480	10.960	19.920	19.920	18.640
$10^7 - 10^8$	13.920	16.880	14.400	5.680	16.400	16.400	15.440

TABLE VI: Comparison of fee ratio, path length, and timelock metrics across Lightning Network Clients for bimodal distribution graph

Attribute	LND1	LND2	CLN	LDK	Eclair_case1	Eclair_case2	Eclair_case3
Fee	0.069%	0.020%	0.055%	0.164%	0.100%	0.100%	0.020%
Path Length	4.463	6.291	4.577	4.489	4.412	4.412	6.580
Timelock	198.387	264.593	190.894	203.937	198.792	198.792	276.539

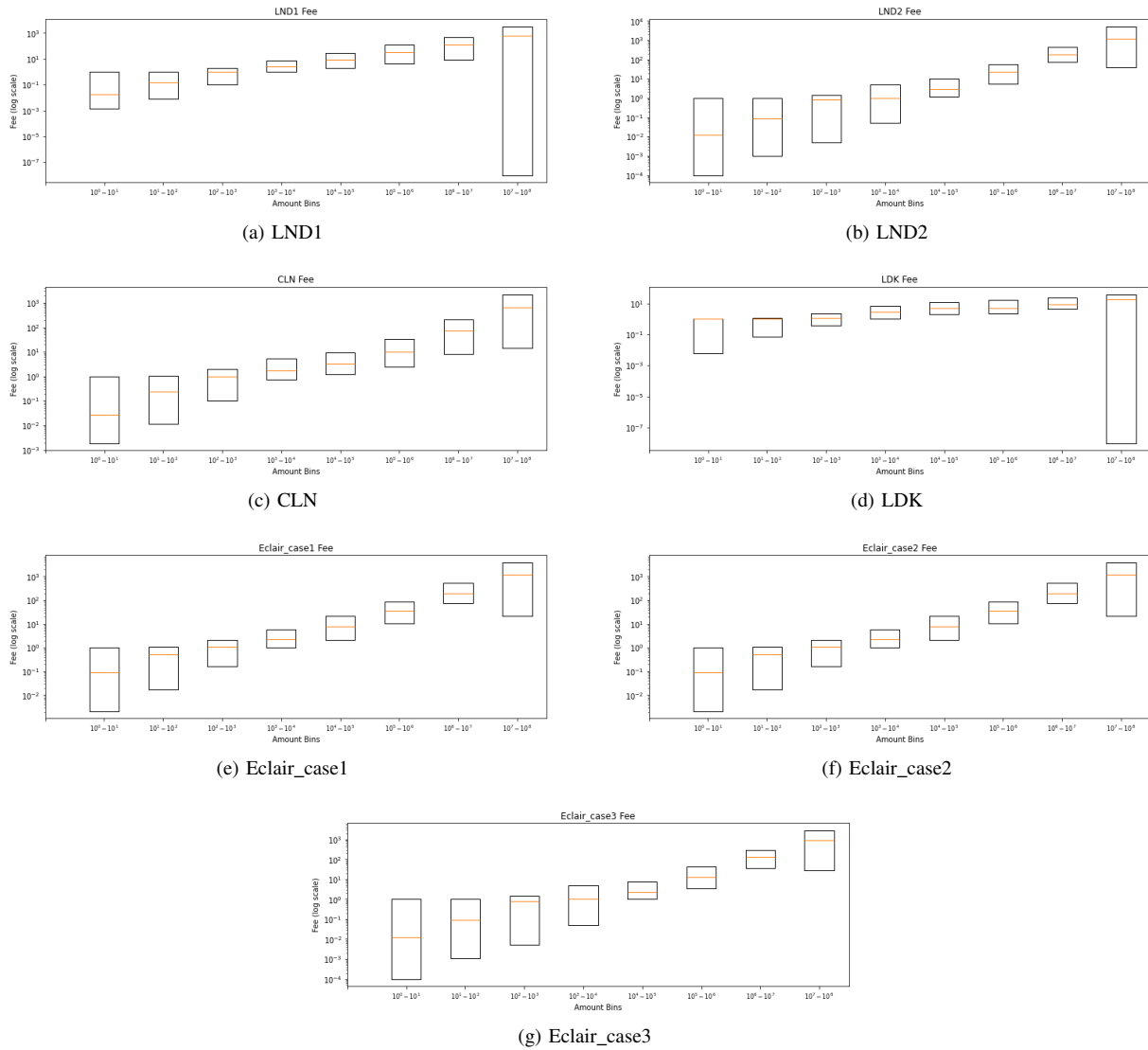


Fig. 3: Fee distribution across transaction amount bins

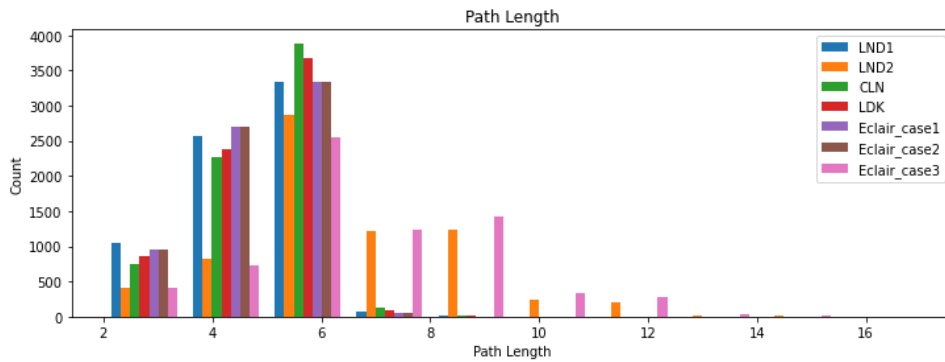


Fig. 4: Distribution of path lengths across Lightning Network clients

TABLE VII: Success rates for amounts in range 10-100 sats across different node category combinations for source and receiver

Source-Receiver	LND1	LND2	CLN	LDK	Eclair_case1	Eclair_case2	Eclair_case3
Well-Well	100	100	100	100	100	100	100
Well-Fair	100	100	100	100	100	100	100
Well-Poor	100	100	100	100	100	100	100
Fair-Well	100	100	100	100	100	100	100
Fair-Fair	100	100	100	100	100	100	100
Fair-Poor	99.394	99.394	99.394	99.394	99.394	99.394	99.394
Poor-Well	98.387	98.387	98.387	98.387	98.387	98.387	98.387
Poor-Fair	98.204	98.204	98.204	98.204	98.204	98.204	98.204
Poor-Poor	96.774	96.774	96.774	96.774	96.774	96.774	96.774

TABLE VIII: Success rates for amounts in the range of 10^3 - 10^4 sats across different node category combinations for source and receiver

Source-Receiver	LND1	LND2	CLN	LDK	Eclair_case1	Eclair_case2	Eclair_case3
Well-Well	97.60	96.80	96	99.20	96.80	96.80	96.80
Well-Fair	88.623	89.222	88.024	91.617	91.617	91.617	90.419
Well-Poor	90.4	90.4	92	90.4	91.2	91.2	88.8
Fair-Well	83.832	86.228	84.431	86.228	83.832	83.832	85.030
Fair-Fair	73.653	85.629	76.647	84.431	80.240	80.240	85.629
Fair-Poor	74.251	83.234	77.844	81.437	76.647	76.647	82.036
Poor-Well	89.6	89.6	89.6	89.6	90.4	90.4	90.4
Poor-Fair	80.838	91.617	86.826	90.419	84.431	84.431	91.018
Poor-Poor	89.6	88	88.8	89.6	89.6	89.6	86.4

TABLE IX: Success rates for amounts in the range of 10^5 - 10^6 sats across different node category combinations for source and receiver

Source-Receiver	LND1	LND2	CLN	LDK	Eclair_case1	Eclair_case2	Eclair_case3
Well-Well	40.80	64.80	50.40	46.40	53.60	53.60	60.80
Well-Fair	27.108	39.157	31.325	30.723	36.145	36.145	39.157
Well-Poor	48	62.4	52.8	51.2	61.6	61.6	64
Fair-Well	22.289	37.952	28.916	33.735	32.530	32.530	34.940
Fair-Fair	12.048	16.867	12.651	13.253	15.663	15.663	15.663
Fair-Poor	18.675	28.313	22.892	21.687	27.711	27.711	25.904
Poor-Well	45.6	60	51.2	43.2	56.8	56.8	53.6
Poor-Fair	18.072	27.108	23.494	27.108	27.108	27.108	26.506
Poor-Poor	28.8	40.8	34.4	33.6	33.6	33.6	40

across multiple bins.

In comparison to the uniform distribution case results in Table III, success rates in the bimodal distribution graph are significantly lower. This decline in success rates is attributed to the bimodal distribution of channel liquidity. As the payment amount increases, it becomes challenging to identify reliable routes for payment delivery due to the scarcity of available liquidity. Moreover, Table VI reveals a substantial increase in the fee ratio across all LN clients under the bimodal distribution scenario. Despite the bimodal distribution graph, Eclair_case3 still achieves the lowest fee ratio. In addition, Eclair_case1 and Eclair_case2 display the shortest path lengths, while CLN maintains the lowest overall timelock.

As discussed earlier in this section, evaluating routing across different node categories is important. Therefore, we simulated transactions on the uniform distribution graph, by selecting nodes from well, fairly, and poorly connected node categories, resulting in a total of 9 experiments, each consisting of 1,000 transactions. These experiments covered all possible combinations of node categories by selecting source and destination

nodes from the three connectivity levels. Payment amounts for each transaction were determined using the previously mentioned strategy.

In all possible node category combinations for selecting source and receiver nodes, routing clients achieve varying success rates in different bins, as illustrated in Table VII, Table VIII and Table IX.

Since we classify nodes based on both the number of channels and their total capacity, fairly connected nodes, with capacities ranging between 10^4 and 10^6 , can only accommodate transaction amounts less than 10^6 , resulting in bins ranging from 1 to 10^6 . In contrast, well and poorly connected nodes may have capacities exceeding 10^6 , enabling transaction amounts from bins ranging from 1 to 10^8 . Therefore, to ensure a meaningful comparison of results, we compared success rates within each bin separately. From Table VII, it can be observed that for small payment amounts (10-1000 sats), the success rates are high across all node category combinations. However, notably, for combinations involving poorly connected nodes, the success rates are relatively lower.

Overall from Table VIII and Table IX, across all routing clients, we observed that well-connected nodes exhibit high success rates, along with low fees, low delay, and short path lengths. Fairly connected nodes, on the other hand, provide lower success rates, charge moderate fees, with moderate delay and path length. In case of poorly connected nodes, the success rate surpasses that of fairly connected nodes. This is attributed to poorly connected nodes having substantial capacity, enabling successful payment routing despite having fewer channels. However, it should be noted that poorly connected nodes typically impose high fees, experience high delay, and have longer path lengths which are undesirable for efficient routing.

From the results of these connectivity level routing evaluation experiments, we found that LND2 consistently delivers high success rates across all node categories, while LND1 emerges as a poor performer, especially across all node category combinations in Table IX, compared to all other clients. LDK demonstrates moderate reliability, across most of the node combinations. In situations where nodes are poorly connected, CLN emerges as a strong contender due to its competitive performance. Eclair_case3 exhibits higher success rates for well-connected nodes, while Eclair_case1 and Eclair_case2 record competitive success rates across all node combinations. Notably, even within these experiments, Eclair_case3 consistently provides paths with the lowest fees, though with the highest path length and timelock. Conversely, LDK yields paths with the highest fees for lower payment amounts. Eclair_case1 and Eclair_case2 offers shorter path lengths, whereas CLN yields paths with the lowest delay.

Analyzing the results from all our experiments and interpreting them using the weight functions from Section VI, several insights can be inferred. The high success rates exhibited by LND2 across various experiments can potentially be attributed to its adept modeling of success probabilities using bimodal estimators. To further improve the performance of LND2, it will be important to fine-tune the liquidity broadening scale s in (16).

LND1's low success rate can be attributed to the apriori estimation of the success probability, which assumes a base success likelihood of 0.6. This assumption, along with default values for the constants c_o and s_o in (13), might not yield reliable paths with. Moreover, this model takes into account historical payment attempts to adjust the channel-wise success probability as described in Equation (9). However, in our simulation, we did not consider historical attempts when computing the success probabilities, which might have contributed to the low success rate.

Examination of the weight function (32) employed by Eclair_case3 reveals a tendency to favor paths with lower fees, as evidenced by the relatively diminished influence of other design elements within the weight function, which are assigned lower cost, and consequently contribute less weight compared to fees. This trend is consistent with the observed outcomes, indicating that Eclair_case3 consistently offers paths characterized by lower fees.

The efficacy of CLN in providing paths with low timelock can also be attributed to the design of its weight function, which prioritizes paths with lower timelock. Additionally, CLN's competitive performance with poorly connected nodes can be linked to $capacityBias_e$ in (17), as it penalizes channels where a significant portion of channel capacity is utilized. This design feature enables CLN to perform more effectively among nodes with large capacity. In our experimental setup, some poorly connected nodes possess channels with substantial capacity, CLN's weight function incentivizes such channels. Consequently, resulting in competitive performance in such scenarios.

Finally, LDK's decline in reliability for larger amounts can be attributed to the weight function (19) which prioritizes paths with lower fees over higher reliability. The higher fee ratio for small payment amounts in LDK may result from the weight function favoring paths with lower HTLC minimums rather than lower fees as illustrated in Section VI-C.

VIII. LIMITATIONS

In our simulation model, we do not consider the historical payment attempts to update the channel-wise success probability. In the event of failure, the success probability of the failed channel is not taken to zero, as it is in LND1.

Furthermore, our model neither has the capability to record historical liquidity estimations like channel upper bound and lower bounds, as in LDK, nor does it have the capability to record the previous success and failure amounts in the channel, as is the case in LND.

Our model does not consider all the side constraints during pathfinding. Specifically, we do not consider constraints on timelock, path length, and fees.

This limitation may introduce slight variations in the results observed in real Lightning Network routing. Additionally, we used default values for design elements that are constants. Varying these values could yield different results.

IX. CONCLUSION

In this study, we assess the empirical performance of four prominent Lightning Network clients: LND, CLN, LDK, and Eclair, across various metrics including success rate, fee ratio, path length, and timelock. Our experiments reveal that LND demonstrates superior success rates, which can be attributed to its detailed modeling of success probabilities and its larger emphasis on these in the implied path cost. Conversely, LDK demonstrates moderate reliability but suboptimal fee performance for smaller payments, while Eclair distinguishes itself by offering paths with low fees. Additionally, CLN stands out for providing paths with minimal timelock, which is aligned with its weight function modelling which is designed to prioritize timelock minimization.

We find that the connectivity level of nodes significantly influences the selection of an appropriate path. Depending on the node's connectivity level and the desired performance metric optimization, the selection of the appropriate weight function or routing client becomes crucial.

Furthermore, we observe that certain path cost modeling, while reasonable from a modeling perspective, can harm the performance of the pathfinding algorithm, and simple, modifications to standard shortest path algorithms such as Dijkstra’s algorithm do not always return the expected, optimal solution, in particular, in the case of LND’s cost function. We also observe that the imposition of side constraints (see (8) and Table I) imposes potentially severe difficulties for the pathfinding process, as the underlying problem becomes a constrained shortest-path problem, which is \mathcal{NP} -complete and thus cannot be guaranteed to be solved optimally in practice for all but small graph instances.

We hope that the insights of this study motivate future developments in designing better weight functions which, dependent on the desired properties of the resulting path, can deliver better trade-offs between payment reliability, routing fees and other desired properties. We expect that there is room for substantial improvements in future work. From an algorithmic side, we conclude that it is worthwhile to consider more sophisticated algorithms than Dijkstra’s algorithm (or its ad-hoc modifications) to improve pathfinding both in terms of computational efficiency (which corresponds to payment latency) and solution quality (which corresponds to routing fees and payment reliability).

Finally, while beyond the scope of this study, we note that the insights gained in this study are also relevant for future improvements in multi-part payment pathfinding algorithms, as those algorithms are based on the solution of minimum cost flow problems, which are a generalization of shortest path problems. The choice of an appropriate channel-specific weight/cost function likewise significantly influences the solution quality in multi-part pathfinding.

REFERENCES

- [1] Satoshi Nakamoto. Bitcoin: A peer-to-peer electronic cash system. <https://bitcoin.org/bitcoin.pdf>, 2008.
- [2] Vitalik Buterin. Sharding FAQ: This sounds like there’s some kind of scalability trilemma at play. What is this trilemma and can we break through it? https://vitalik.eth.limo/general/2017/12/31/sharding_faq.html, 2017. (Accessed: Sep. 16, 2024).
- [3] Taishi Nakai, Akira Sakurai, Shiori Hironaka, and Kazuyuki Shudo. A Formulation of the Trilemma in Proof of Work Blockchain. *IEEE Access*, doi:10.1109/ACCESS.2024.3410025, 2024.
- [4] Joseph Poon and Thaddeus Dryja. The Bitcoin Lightning Network: Scalable Off-Chain Instant Payments. Available at <https://lightning.network/lightning-network-paper.pdf>, 2016.
- [5] Overview — Builder’s Guide — docs.lightning.engineering. <https://docs.lightning.engineering/the-lightning-network/overview>.
- [6] Andreas M. Antonopoulos, Olaoluwa Osuntokun, and René Pickhardt. *Mastering the Lightning Network*. ” O’Reilly Media, Inc.”, 2021.
- [7] Giovanni Di Stasi, Stefano Avallone, Roberto Canonico, and Giorgio Ventre. Routing payments on the lightning network. In *2018 IEEE International Conference on Internet of Things (IThings) and IEEE Green Computing and Communications (GreenCom) and IEEE Cyber, Physical and Social Computing (CPSCom) and IEEE Smart Data (SmartData)*, pages 1161–1170. IEEE, 2018.
- [8] Satwik Prabhu Kumble and Stefanie Roos. Comparative analysis of lightning’s routing clients. In *2021 IEEE International Conference on Decentralized Applications and Infrastructures (DAPPS)*, pages 79–84. IEEE, 2021.
- [9] René Pickhardt. Evaluating Path finding Strategies on the Lightning Network — renepickhardt. <https://medium.com/@renepickhardt/evaluating-path-finding-strategies-on-the-lightning-network-238fe2fdf3d6>.
- [10] GitHub - lightningnetwork/lnd: Lightning Network Daemon — github.com. <https://github.com/lightningnetwork/lnd/tree/master>.
- [11] GitHub - ElementsProject/lightning: Core Lightning — Lightning Network implementation focusing on spec compliance and performance — github.com. <https://github.com/ElementsProject/lightning>.
- [12] GitHub - lightningdevkit/rust-lightning: A highly modular Bitcoin Lightning library written in Rust. It’s rust-lightning, not Rusty’s Lightning! — github.com. <https://github.com/lightningdevkit/rust-lightning>.
- [13] GitHub - ACINQ/eclair: A scala implementation of the Lightning Network. — github.com. <https://github.com/ACINQ/eclair/tree/master>.
- [14] René Pickhardt, Sergei Tikhomirov, Alex Biryukov, and Mariusz Nowostawski. Security and Privacy of Lightning Network Payments with Uncertain Channel Balances. *arXiv preprint, arXiv:2103.08576*, 2021.
- [15] George Kappos, Haaron Yousaf, Ania Piotrowska, Sanket Kanjalkar, Sergi Delgado-Segura, Andrew Miller, and Sarah Meiklejohn. An empirical analysis of privacy in the lightning network. In *Financial Cryptography and Data Security: 25th International Conference, FC 2021, Virtual Event, March 1–5, 2021, Revised Selected Papers, Part 1* 25, pages 167–186. Springer, 2021.
- [16] Saar Tochner, Aviv Zohar, and Stefan Schmid. Route hijacking and dos in off-chain networks. In *Proceedings of the 2nd ACM Conference on Advances in Financial Technologies*, pages 228–240, 2020.
- [17] Arad Kotzer and Ori Rottenstreich. Braess paradox in layer-2 blockchain payment networks. In *2023 IEEE International Conference on Blockchain and Cryptocurrency (ICBC)*, pages 1–9. IEEE, 2023.
- [18] Gustavo F Camilo, Gabriel Antonio F Rebello, Lucas Airam C de Souza, Miguel Elias M Campista, and Luís Henrique MK Costa. Profitpilot: Enabling rebalancing in payment channel networks through profitable cycle creation. *IEEE Transactions on Network and Service Management*, 2024.
- [19] Gustavo F. Camilo, Gabriel Antonio F. Rebello, Lucas Airam C. de Souza, Maria Potop-Butucaru, Marcelo D. Amorim, Miguel Elias M. Campista, and Luís Henrique MK Costa. Topological evolution analysis of payment channels in the lightning network. In *2022 IEEE Latin-American Conference on Communications (LATINCOM)*, pages 1–6. IEEE, 2022.
- [20] Yuwei Guo, Jinfeng Tong, and Chen Feng. A measurement study of bitcoin lightning network. In *2019 IEEE International Conference on Blockchain (Blockchain)*, pages 202–211. IEEE, 2019.
- [21] Pavel Prihodko, Slava Zhigulin, Mykola Sahnno, Aleksei Ostrovskiy, and Olaoluwa Osuntokun. Flare: An approach to routing in lightning network. *White Paper*, 144, 2016.
- [22] Vibhaalakshmi Sivaraman, Shaileshh Bojja Venkatakrishnan, Kathleen Ruan, Parimarjan Negi, Lei Yang, Radhika Mittal, Giulia Fanti, and Mohammad Alizadeh. High throughput cryptocurrency routing in payment channel networks. In *17th USENIX Symposium on Networked Systems Design and Implementation (NSDI 20)*, pages 777–796, 2020.
- [23] Vivek Bagaria, Joachim Neu, and David Tse. Boomerang: Redundancy improves latency and throughput in payment-channel networks. In *International Conference on Financial Cryptography and Data Security*, pages 304–324. Springer, 2020.
- [24] Base AMP by rustyussell · Pull Request #643 - lightning/bolts — github.com. <https://github.com/lightning/bolts/pull/643>.
- [25] René Pickhardt and Stefan Richter. Optimally Reliable & Cheap Payment Flows on the Lightning Network. *arXiv preprint, arXiv:2107.05322*, 2021.
- [26] Sonbol Rahimpour and Majid Khabbazian. Spear: fast multi-path payment with redundancy. In *Proceedings of the 3rd ACM Conference on Advances in Financial Technologies*, pages 183–191, 2021.
- [27] lnd/routing/pathfind.go at master · lightningnetwork/lnd — github.com. <https://github.com/lightningnetwork/lnd/blob/master/routing/pathfind.go>.
- [28] lightningdevkit/rust-lightning · ElementsProject/lightning — github.com. <https://github.com/ElementsProject/lightning/blob/master/common/dijkstra.c>.
- [29] rust-lightning/lightning/src/routing/router.rs at main · lightningdevkit/rust-lightning — github.com. <https://github.com/lightningdevkit/rust-lightning/blob/main/lightning/src/routing/router.rs>.
- [30] eclair/eclair-core/src/main/scala/fr/acinq/eclair/router/Graph.scala at master · ACINQ/eclair — github.com. <https://github.com/ACINQ/eclair/blob/master/eclair-core/src/main/scala/fr/acinq/eclair/router/Graph.scala>.
- [31] Thomas H. Cormen, Charles E. Leiserson, Ronald L. Rivest, and Clifford Stein. *Introduction to Algorithms*. MIT Press, 2022.

- [32] Joost Jager. Commit "routing: use probability source in path finding" · lightningnetwork/lnd — github.com. <https://github.com/lightningnetwork/lnd/blob/758ae6fbecfca6809bf6d51427717245c3c777db/routing/pathfind.go#L1047-L1079>, 2019. (Accessed: Oct. 12, 2024).
- [33] Clearing the Paths: A Deep Dive into LND's Pathfinding Mechanism — lightning.engineering. <https://lightning.engineering/posts/2024-04-11-pathfinding-1/>.
- [34] Ravindra K. Ahuja, Thomas L. Magnanti, and James B. Orlin. *Network Flows*. Prentice Hall, 1993.
- [35] Blazing the Trails: Improving LND Pathfinding Reliability — lightning.engineering. <https://lightning.engineering/posts/2024-05-23-pathfinding-2/>.
- [36] Pathfinding: take channel capacity into account · Issue #5988 · lightningnetwork/lnd — github.com. <https://github.com/lightningnetwork/lnd/issues/5988#issuecomment-1131234858>.
- [37] René Pickhardt. The power of valves for better flow control, improved reliability & lower expected payment failure rates on the Lightning network. *BitMEX Research Blog*, 2022. Available at https://blog.bitmex.com/the-power-of-htlc_maximum_msat-as-a-control-valve-for-better-flow-control-improved-reliability-and-lower-expected-payment-failure-rates-on-the-lightning-network/ (Accessed: Oct. 15, 2024).
- [38] E. W. Dijkstra. A note on two problems in connexion with graphs. *Numerische Mathematik*, 1(1):269–271, 1959.
- [39] Ellis L. Johnson. On shortest paths and sorting. In *Proceedings of the ACM Annual Conference-Volume 1*, pages 510–517, 1972.
- [40] <https://www.rene-pickhardt.de/listchannels20220412.json>.
- [41] Dimitri Bertsekas. *Network Optimization: Continuous and Discrete Models*, volume 8. Athena Scientific, 1998.
- [42] Ying Xiao, Krishnaiyan Thulasiraman, Guoliang Xue, Alpár Jüttner, and S Arumugam. The constrained shortest path problem: algorithmic approaches and an algebraic study with generalization. *AKCE International Journal of Graphs and Combinatorics*, 2(2):63–86, 2005.
- [43] Stefan Irnich and Guy Desaulniers. Shortest path problems with resource constraints. In *Column generation*, pages 33–65. Springer, 2005.
- [44] Luigi Di Puglia Pugliese and Francesca Guerriero. A survey of resource constrained shortest path problems: Exact solution approaches. *Networks*, 62(3):183–200, 2013.
- [45] Abderrahim Bendahi and Adrien Fradin. On constrained and k shortest paths. *arXiv preprint, arXiv:2408.00899*, 2024.
- [46] Jin Y. Yen. Finding the k shortest loopless paths in a network. *management Science*, 17(11):712–716, 1971.
- [47] Eric Bouillet, Georgios Ellinas, Jean-Francois Labourdette, and Ramu Ramamurthy. *Path Routing in Mesh Optical Networks*. John Wiley & Sons, 2007.
- [48] GitHub - lightning/bolts: BOLT: Basis of Lightning Technology (Lightning Network Specifications) — github.com. <https://github.com/lightning/bolts>.
- [49] NetworkX: NetworkX documentation — networkx.org. <https://networkx.org/>.